VOLUME 23 NUMBER 8

ACCOUNTS OF CHEMICAL RESEARCH®

AUGUST 1990



# Electronic Structures and Reactivities of Metal Cluster Complexes

WILLIAM C. TROGLER

*Department of Chemistry, D-006, University of California at San Diego, La Jolla, California 92093-0506*

*Received December 29, 1989 (Revised Manuscript Received March 28, 1990)*

The effect of metal–metal interactions on the physical properties and reactivity of transition-metal cluster complexes has been an area of interest in our laboratory for over a decade. At the time we began these studies, the nature of metal–metal interactions in dinuclear complexes was well understood; most advanced undergraduate inorganic texts contain a discussion of metal–metal $\sigma$, $\pi$, and $\delta$ bonds. The degree of complexity increases rapidly as one considers clusters of three, four, and six metals so that a qualitative discussion of the bonding and its impact on physical properties becomes difficult. One question we hoped to address was whether an energy-band approach to small molecular clusters offered any advantage in understanding their electronic structures. Theoretical studies of pure metallic clusters suggest that as few as 40–80 metal atoms result in some properties similar to the bulk metal.[1]

Another point of concern was the effect of delocalized metal–metal bonding on the thermal and photochemical reactivity of polynuclear complexes. Photochemical metal–metal bond homolysis in dinuclear complexes was well established and shown to result from excitation of a $\sigma \rightarrow \sigma^*$ electronic transition;[2] however, the situation for larger clusters was more complex.[3] In particular, the factors that control metal–metal bond homolysis vs metal–ligand bond cleavage in both thermal and photochemical reactions were topics that interested us. Since polynuclear compounds often serve as delocalized pools of electrons for redox chemistry (e.g., ferredoxins), the consequences of delocalized bonding on cluster redox properties and reactivity provided another question to be examined.

**Theoretical Methods.** Electron counting rules have proved to be extremely valuable for predicting cluster geometries and stabilities.[4] For our goal of understanding spectroscopic properties, charge distributions, and reactivities, we sought a first principles theory capable of providing such information. To us the best compromise between theoretical rigor and the ability to perform computations in a reasonable time was the X$\alpha$ procedure.[5] In this approximate method one replaces the exchange potential operator, $K_j$, in the Hartree–Fock (HF) equations with the expression of eq 1. This equation describes the exchange energy for a

$$[\mathrm{KX}\alpha\uparrow(1)] = -6\alpha\left[\frac{3}{4\pi}\rho\uparrow(1)\right]^{1/3} \qquad (1)$$

free-electron gas, which depends only on the electron density distribution, $\rho$, and avoids the calculation of time-consuming exchange integrals. The parameter $\alpha(\sim 0.7)$ can be determined by fitting atomic calculations to the HF results. It has been argued[5] that this approximation incorporates correlation between electrons. This may have some validity in view of the success the X$\alpha$ method has shown in treating weak metal–metal bonds, such as in $Cr_2(O_2CH)_4$,[6] and in

William C. Trogler, born on December 23, 1952, in Baltimore, MD, is a Professor of Chemistry at the University of California at San Diego. He received B.A. and M.A. degrees from the Johns Hopkins University and studied with Harry Gray at Caltech for his Ph.D. He was a member of the chemistry faculty at Northwestern University before joining the department at San Diego. His research interests span physical-mechanistic and catalytic aspects of coordination and organometallic complexes.

(1) Melius, C. F.; Upton, T. H.; Goddard, W. A., III. *Solid State Commun.* **1978**, *238*, 501.
(2) Geoffroy, G. L.; Wrighton, M. S. *Organometallic Photochemistry*; Academic Press: New York, 1979.
(3) Manning, M. C.; Trogler, W. C. *Coord. Chem. Rev.* **1981**, *38*, 89.
(4) Wade, K. *Transition Metal Clusters*; Johnson, B. F. G., Ed.; Wiley: New York, 1981; pp 193–224.
(5) Slater, J. C. *The Self-Consistent Field for Molecules and Solids*; McGraw-Hill: New York, 1974.

0001-4842/90/0123-0239$02.50/0 

diatomic transition-metal species,[7] when compared to more computer intensive HF-CI procedures.

In the Xα approximation several different approaches have been applied to the calculation of the Coulomb potential. In the muffin tin (MT) Xα scheme[5] one assumes a spherically symmetrical potential within touching spheres around each atom. Outside these spheres the potential is constant. This procedure, originally designed for solids,[5] is a poor approximation for molecules with a strong bond (e.g., CO). The scattered wave (SW) method[8] allows the potential spheres to overlap and thereby allows flexibility in the description of the bonding regions. This produces better results for molecular species.[9] We adopted an alternative treatment called the discrete variational method (DV)[10] and were fortunate to engage in a fruitful collaboration with an inventor of the technique[10,11] in applications to organometallic systems. In this procedure one computes the various integrals on a grid of points (usually 300 points/atom) distributed throughout the molecule. The degree of numerical accuracy can be increased by increasing the number of such points (at an expense in computation time). It is still convenient to expand the charge density in spherical harmonics about each atom, and there are several ways to do this. By the use of a spherical wave expansion from an orbital charge population (SCC) analysis[12] one obtains results that we have found to be similar to those of the SW method in a number of trial calculations on mononuclear and dinuclear complexes.[12] A more rigorous procedure is to use an analytical least-squares fit of the molecular charge density with expansion functions localized on atoms, as well as between bonds.[13] This permits one to approach an exact solution of the Xα Hamiltonian.

An important distinction for Xα orbital energies is that they represent the partial derivative of the total energy with respect to the occupation number for that orbital. Therefore, one cannot simply equate an Xα orbital energy diagram with that for a HF calculation. Although this is a disadvantage, because Xα orbital energies cannot be equated with ionization potentials, the problem is solved by the transition-state method.[4] Here one performs the calculation of a hypothetical transition state for a spectroscopic process. For example, to calculate the ionization potential from orbital $\theta_i$, one calculates the energy, $\epsilon_i$, for this orbital with one-half of an electron removed (i.e., for the +0.5 ion). For an electronic transition one removes one-half of an electron from an occupied orbital and promotes it to the appropriate unoccupied orbital. These calculations converge rapidly once the ground-state calculation has been completed and have the advantage of reoptimizing the orbitals for each specific transition. Our experience in transition-metal systems has been that the calculated

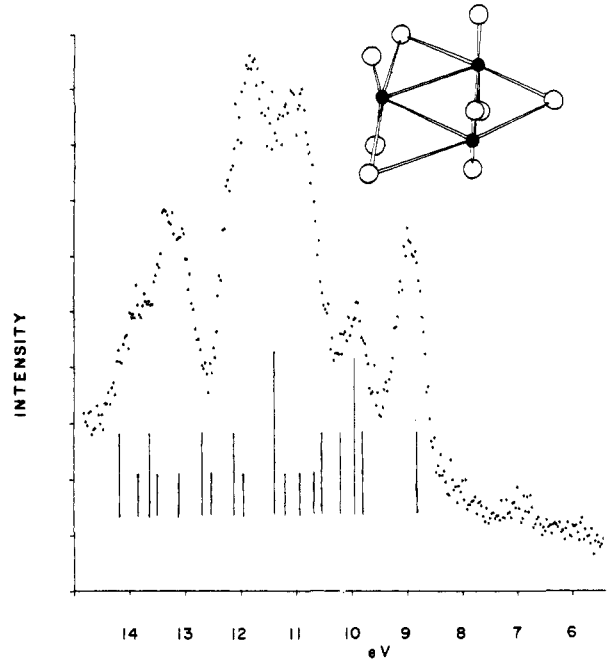


**Figure 1.** Valence photoelectron spectrum of $Re_3Cl_9$ vapor at 800 K. Vertical lines represent predicted ionizations from SCF-Xα-DV calculations. Adapted from ref 14.

energies usually are within 1.0 eV of experimental values. This substantial error is about what one can realistically expect from calculations of many-electron clusters.

**Trinuclear Metal Cluster Complexes.** The first systems we examined, $Re_3Cl_9$[14] and $M_3(CO)_{12}$ (M = Ru and Os),[15] were chosen because of their volatility and high symmetry ($D_{3h}$). This permitted the measurement of gas-phase photoelectron spectra (PES) and simplified the calculations. At the time, it was fortunate that Dr. Joseph Berkowitz of Argonne National Laboratories allowed me to vaporize these compounds into his PES system. It was a challenge to obtain a spectrum before the insulating film of deposited cluster destroyed the resolution of the spectrometer (resulting in a 4-h disassembly and cleaning of the instrument); however, satisfactory spectra were eventually obtained. In Figure 1 is displayed the valence photoelectron spectrum of $Re_3Cl_9$, measured at about 800 K, with vertical lines for the predicted orbital ionization potentials from an Xα calculation. The close correspondence between the peaks in the experimental spectrum and the calculated ionization potentials, as well as the agreement between the absolute energies for the net splitting of the valence electron ionizations (8.9–13.86 eV experiment vs 8.7–14.2 eV calculated), gave us confidence in the merit of the computational approach. A striking feature of the system was the predicted high stability of a cluster three-center σ-bonding orbital, formed by 3d orbitals directed toward the center of the cluster, denoted $\sigma_c$ in Figure 2. A subsequent PES and SCF-Xα-SW study[16] of the same system and the bromide analogue arrived at substantially the same conclusions with the inclusion of relativistic corrections.[17]

(6) Cotton, F. A.; Stanley, G. G. *Inorg. Chem.* **1977**, *16*, 2668.
(7) Delley, B.; Freeman, A. J.; Ellis, D. E. *Phys. Rev. Lett.* **1983**, *50*, 488.
(8) Johnson, K. H. *Annu. Rev. Phys. Chem.* **1975**, *26*, 39.
(9) Norman, J. G., Jr. *J. Chem. Phys.* **1974**, *61*, 4630.
(10) Ellis, D. E.; Painter, G. H. *Phys. Rev. B* **1970**, *2*, 2887.
(11) Trogler, W. C.; Desjardins, S. R.; Solomon, E. I. *Inorg. Chem.* **1979**, *18*, 2131. Trogler, W. C.; Johnson, C. E.; Ellis, D. E. *Inorg. Chem.* **1981**, *20*, 980. Gross, M. E.; Trogler, W. C.; Ibers, J. A. *Organometallics* **1982**, *1*, 732. Manning, M. C.; Holland, G. F.; Ellis, D. E.; Trogler, W. C. *J. Phys. Chem.* **1983**, *87*, 3083. Lee, S. W.; Trogler, W. C. *Inorg. Chem.* **1990**, *29*, 1659.
(12) Rosen, A.; Ellis, D. E. *J. Chem. Phys.* **1976**, *65*, 3629.
(13) Delley, B.; Ellis, D. E. *J. Chem. Phys.* **1982**, *76*, 1949.
(14) Trogler, W. C.; Ellis, D. E.; Berkowitz, J. *J. Am. Chem. Soc.* **1979**, *101*, 5896.
(15) Delley, B.; Manning, M. C.; Ellis, D. E.; Berkowitz, J.; Trogler, W. C. *Inorg. Chem.* **1982**, *21*, 2247.
(16) Bursten, B. E.; Cotton, F. A.; Green, J. C.; Seddon, E. A.; Stanley, G. G. *J. Am. Chem. Soc.* **1980**, *102*, 955.

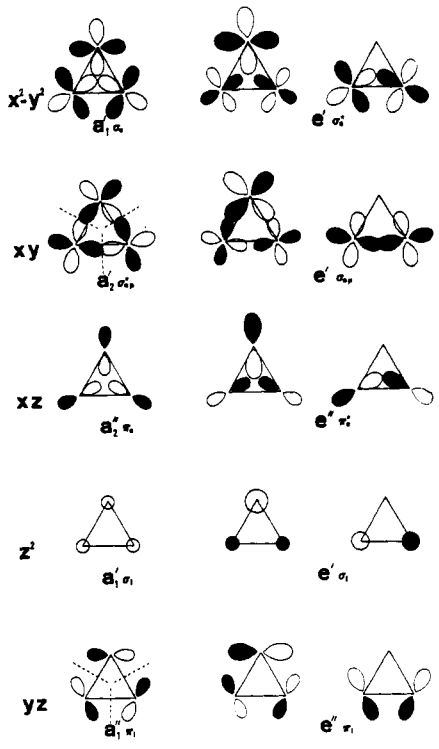


**Figure 2.** Symmetry combinations of metal d orbitals in a trinuclear metal cluster.

In subsequent spectroscopic and theoretical studies of $M_3(CO)_{12}$ clusters, we analyzed[15] metal d-orbital interactions according to the diagram in Figure 2. As for $Re_3Cl_9$, the most stable metal-localized orbital (Figure 3) was the three-center-cluster $\sigma$-bonding orbital, denoted $\sigma_c$ in Figures 2 and 3. Unlike the case of the rhenium cluster system, the $\sigma_c$* orbital was also occupied in the carbonyl systems, along with the degenerate cluster $\pi$ orbitals, denoted $\pi_c$ and $\pi_c$*. These were split about the two $\pi_1$ orbitals of the cluster that engage in $\pi$-back-bonding to the carbonyl groups. Filled metal–metal antibonding orbitals in electron-rich carbonyl clusters can still experience a net stabilization by $\pi$-back-bonding to the carbonyl groups, as shown for the 14e′($\sigma_c$*) orbital in Figure 4. Net metal–metal bonding in the cluster derives from the occupied 15e′ ($\sigma_{cp}$) orbital that resembles a cyclopropane-like edge-bonding orbital. This four-electron $\sigma$-bonding model corresponds well with Pauling's valence-bond description[18] of two edge bonds resonating among three triangular edges in these clusters. The quantitative agreement obtained[15] between the calculated d-orbital splitting and that observed in PES spectra of $Ru_3(CO)_{12}$ and $Os_3(CO)_{12}$ suggests that the model is substantially correct.

It was known that both metal–metal bond cleavage and CO dissociation could occur in the $M_3(CO)_{12}$ clusters on irradiation with ultraviolet light.[19] Therefore, we focused attention on the lowest electronic transitions in these compounds: the dipole-forbidden $10a_1' \rightarrow 6a_2'$ one-electron excitation and the dipole-allowed $15e' \rightarrow 6a_2'$ process. The $10a_1'$ orbital possesses a complex

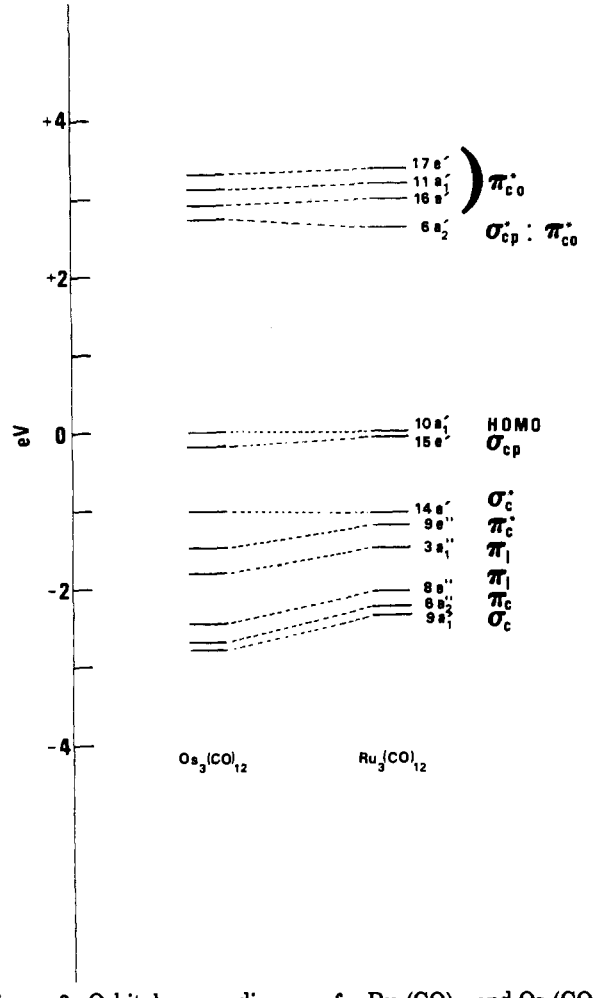


**Figure 3.** Orbital energy diagrams for $Ru_3(CO)_{12}$ and $Os_3(CO)_{12}$ from SCF-X$\alpha$-DV calculations. Reprinted with permission from ref 15. Copyright 1982 American Chemical Society.

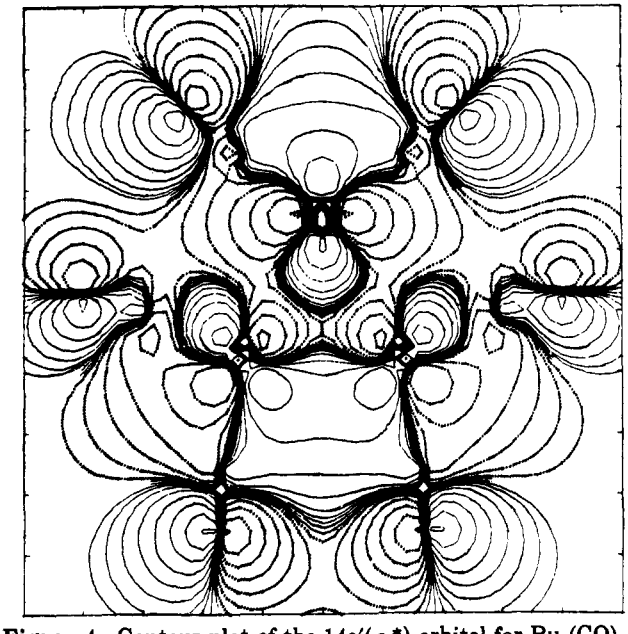

**Figure 4.** Contour plot of the 14e′($\sigma_c$*) orbital for $Ru_3(CO)_{12}$. Reprinted with permission from ref 15. Copyright 1982 American Chemical Society.

mixture of $\sigma_c$ character (30%) from metal-based p orbitals, in addition to axial and equatorial CO $\pi$* character. To analyze the effect of these electronic transitions between highly delocalized orbitals, we employed

(17) Christiansen, P. A.; Ermler, W. C.; Pitzer, K. S. *Annu. Rev. Phys. Chem.* **1985**, *36*, 407.
(18) Pauling, L. *Proc. Natl. Acad. Sci. U.S.A.* **1976**, *73*, 4290.
(19) Desrosiers, M. F.; Wink, D. A.; Trautman, R.; Friedman, A. E.; Ford, P. C. *J. Am. Chem. Soc.* **1986**, *108*, 1917. Ford, P. C. *J. Organomet. Chem.* **1990**, *383*, 339. Bentsen, J. G.; Wrighton, M. S. *J. Am. Chem. Soc.* **1987**, *109*, 4518. Bentsen, J. G.; Wrighton, M. S. *J. Am. Chem. Soc.* **1987**, *109*, 4530 and references therein.

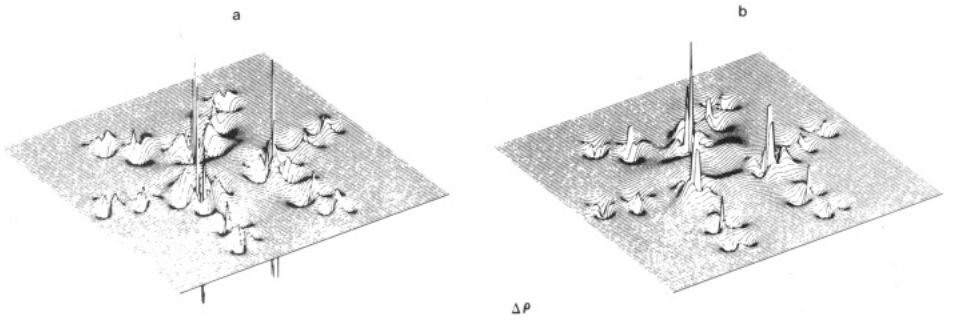


**Figure 5.** Difference electron density plots for the (a) $10a_1' \rightarrow 6a_2'$ and (b) $15e' \rightarrow 6a_2'$ electronic transitions of $Ru_3(CO)_{12}$ in the $Ru_3(CO)_6$ plane. The large spike-like features represent noise in the subtraction of core density at Ru, which serves to mark the Ru atom locations.

a difference density analysis. Here one subtracts the total electron density distribution in the ground state from that in the excited state. The raised contours show where electron density increases after electronic excitation, and the depressed contours show where the electron density has decreased. These three-dimensional plots, shown in Figure 5, reveal a distinct difference between the two excited states. Noise wells from differences in core densities mark the location of the three Ru atoms and six CO ligands in the plane of the triangular cluster core. The important bonding regions lie at the center of the $Ru_3$ triangle and between the Ru and CO ligands. In the first case ($10a_1' \rightarrow 6a_2'$) little disruption of electron density in the triangular core is observed, while the $15e' \rightarrow 6a_2'$ transition shows a large depression in bonding electron density at the center of the $Ru_3$ triangle.

This conclusion is partially supported by the resonance Raman effect observed when the lowest dipole-allowed ($15e' \rightarrow 16a_2'$) electronic transitions in $Ru_3(CO)_{12}$ and $Os_3(CO)_{10}[PPh_2(neomenthyl)]_2$ were excited. Both the $a_1'$ (Ru, 185 $cm^{-1}$; Os, 190 $cm^{-1}$) and the Jahn–Teller-active e′ (Ru, 130 $cm^{-1}$; Os, 140 $cm^{-1}$) metal–metal stretching frequencies exhibit a 2–5-fold intensity enhancement. Since only degenerate excited states can undergo a Jahn–Teller distortion, the enhancement of the Jahn–Teller-active mode supports an assignment of the lowest allowed electronic transition as a degenerate metal-localized $\sigma \rightarrow \sigma^*$ excitation. Resonance-enhanced vibrations correspond to the bonds most disturbed in the resonant excited state. Previous MCD studies also were consistent with the presence of a low-lying dipole-allowed degenerate excited state of predicted metal–metal antibonding character.[20]

The calculated changes in Ru–CO bonding follow an opposite pattern. In $10a_1' \rightarrow 6a_2'$ a double valley develops (Figure 5) between the Ru and CO groups, which represents a loss in $\pi$-bonding density; however, the Ru–CO bonding is relatively undisturbed (i.e., flat) for the $15e' \rightarrow 16a_2'$ difference electron density plot. The presence of these two closely spaced excited states, one metal–metal antibonding and the other metal–CO antibonding, may explain the competing metal–metal bond and metal–CO bond cleavage that occurs on photochemical excitation. This suggestion has been supported by several photochemical studies.[19]

**Tetranuclear Metal Cluster Compounds.** The complexity of tetranuclear cluster complexes leads to a further lowering of resolution in the spectroscopic information obtained, and one relies more heavily on computational methods as a guide. Thermal instability and a lack of volatility preclude gas-phase PES measurements for most systems. A problem with the molecular orbital approach (Figure 6) is that one becomes inundated by information that provides little chemical insight. For these reasons we initially examined bare $M_4$ clusters of iron, cobalt, and nickel.[21] Molecular beam technology has permitted such compounds to be prepared and characterized spectroscopically in the gas phase.[22] These naked metal clusters were predicted to be highly magnetic by the spin-polarized SCF-X$\alpha$-DV calculations with 12, six, and two unpaired electrons, respectively. The calculated exchange splittings of the spin-up and spin-down d orbitals also decreased (2.68, 1.60, and 0.56 eV, respectively) in this series. The Fe and Ni complexes, which contain singly occupied $t_2$ and $t_1$ levels, should undergo Jahn–Teller distortion to $C_{3v}$ or lower symmetry structures. Extensive mixing of metal 4s and 4p character into the metal–metal bonding orbitals was observed, which agreed with previous Hückel calculations.[23] Such hybridization also occurs in the coordinatively saturated $Co_4(CO)_{12}$ system.

The $Co_4(CO)_{12}$ complex possesses a diamagnetic ground state, as do the Rh and Ir analogues (Figure 6).[24] Comparisons within this series are complicated by the

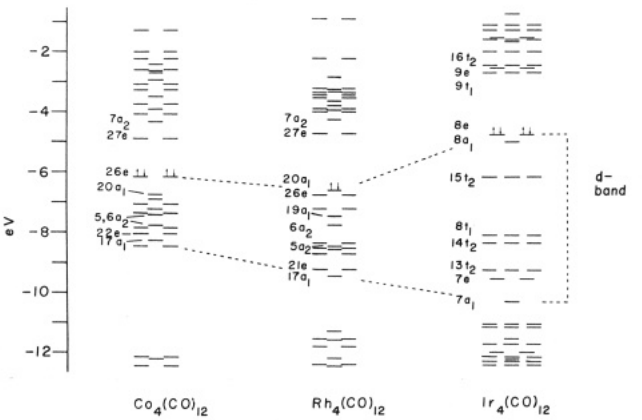


**Figure 6.** Orbital energy diagrams for $M_4(CO)_{12}$ clusters from SCF-X$\alpha$-DV calculations. Reprinted with permission from ref 24. Copyright 1987 American Chemical Society.

(20) Tyler, D. R.; Levenson, R. A.; Gray, H. B. *J. Am. Chem. Soc.* **1978**, *100*, 7888.

(21) Holland, G. F.; Ellis, D. E.; Trogler, W. C. *J. Chem. Phys.* **1985**, *83*, 3507.

(22) Andres, R. P.; Averback, R. S.; Brown, W. L.; Brus, L. E.; Goddard, W. A., III; Kaldor, A.; Louie, S. G.; Moscovits, M.; Peercy, P. S.; Riley, S. J.; Spaepen, F.; Wang, Y. *J. Mater. Res.* **1989**, *4*, 704.

(23) Hoffmann, R.; Schilling, B. E. R.; Bau, R.; Kaesz, H. D.; Mingos, D. M. P. *J. Am. Chem. Soc.* **1978**, *100*, 6088. Schilling, B. E. R.; Hoffmann, R. *J. Am. Chem. Soc.* **1979**, *101*, 3456.

(24) Holland, G. F.; Ellis, D. E.; Tyler, D. R.; Gray, H. B.; Trogler, W. C. *J. Am. Chem. Soc.* **1987**, *109*, 4276.

**Table I**
**Physical Data for Tetranuclear Metal Cluster Complexes**

| complex | redn:[a] $E^{\circ\prime}$ or $E_{pc}$, V | oxidn:[a] $E^{\circ\prime}$ or $E_{pa}$, V | calcd $M_4$ core charge[b] | $M_{ap}$–$M_{ba}$, Å | $M_{ba}$–$M_{ba}$, Å | $\sigma \rightarrow \sigma^*$ λ, nm ($\epsilon$, $M^{-1}$ $cm^{-1}$)[j] | highest $\nu_{CO}$, $cm^{-1}$ |
|---|---|---|---|---|---|---|---|
| $Co_4(CO)_{12}$ | −0.12* | +1.7* | +3.11 | 2.492[c] | 2.492 | 375 (19 000) | 2103[k] |
| $Co_4(CO)_9$(tripod) | −0.78 | +0.94 | +2.41 | 2.540[d] | 2.457 | 380 (11 800) | 2050[f] |
| $(\eta\text{-}MeC_6H_5)Co_4(CO)_9$ | −0.59 | +1.2* | +2.58 | 2.485[e] | 2.457 | 385 (11 800) | 2078[l] |
| $(\eta\text{-}MeC_6H_5)Co_4(CO)_6$(tripod) | −1.21 | +0.39 | +1.80 | 2.472[f] | 2.447 | 380 (11 200) | |
| $(\eta\text{-}C_6Me_6)Co_4(CO)_6$(tripod) | −1.18 | +0.45* | | | | 385 (14 300) | 1980[j] |
| $Rh_4(CO)_{12}$ | −0.80* | | +5.39 | 2.732[g] | | 303 (16 600) | 2101[l] |
| $Rh_4(CO)_9$(tripod) | −1.14 | | | | | 380 (13 000) | 2060[m] |
| $Ir_4(CO)_9$(tripod) | −1.82* | | | 2.684[h] | | 342 (4400) | 2064[n] |
| $Ir_4(CO)_{12}$ | | | +5.40 | 2.693[i] | 2.693 | 321 (7500) | 2071[o] |

[a] Potentials represent $E_{1/2}$ vs an Ag wire pseudoreference at 22 °C from cyclic voltammetry; peak potentials for chemically irreversible couples are indicated by an asterisk. The potential of the ferrocene/ferrocenium couple is +0.47. Potentials are for 0.2 M tetrabutylammonium tetrafluoroborate/$CH_2Cl_2$ solutions, except for $Co_4(CO)_{12}$ and $Rh_4(CO)_{12}$ measured in THF. Data from refs 24 and 26. [b] Values represent the volume-integrated charge in electrons per molecule for the four metal atoms from refs 24 and 26. [c] Carre, F. H.; Cotton, F. A.; Frenz, B. A. *Inorg. Chem.* **1976**, *15*, 380. [d] Darensbourg, D. J.; Zalewski, D. J.; Delord, T. J. *Organometallics* **1984**, *3*, 1210. [e] Reference 28b. [f] Bird, P. H.; Fraser, A. R. *J. Organomet. Chem.* **1974**, *73*, 103. [g] Wei, C. H. *Inorg. Chem.* **1969**, *8*, 2384. [h] Clucas, J. A.; Harding, M. M.; Nicholls, B. S.; Smith, A. K. *J. Chem. Soc., Chem. Commun.* **1984**, 319. [i] Churchill, M. R.; Hutchinson, J. P. *Inorg. Chem.* **1978**, *17*, 3528. [j] References 24 and 26. [k] Noack, K. *Helv. Chim. Acta* **1962**, *45*, 1847. [l] Reference 26. [m] Martinengo, S.; Giordano, G.; Chini, P. *Inorg. Synth.* **1980**, *20*, 209. [n] Reference 54. [o] Chaston, S. H. H.; Stone, F. G. A. *Chem. Commun.* **1967**, 964.

change in structure from $C_{3v}$ (three edge-bridging CO's on a triangular face of the $M_4$ tetrahedron) to $T_d$ (all terminal carbonyls) that occurs on progressing from Rh to Ir. With this caveat, one trend evident from the MO diagrams of Figure 6 is the increase in the energy splitting of the occupied band of d orbitals on descending the periodic table. This can be attributed in part to the increased strength of metal–metal bonding with increasing atomic number. The greatest change occurs on going from the second to the third row of the transition elements. The lowest unoccupied orbital in the $M_4(CO)_{12}$ clusters, 27e or $9t_1$, has the character of a $\sigma_c^*$ orbital with respect to bonding in a triangular face of the cluster. Thus, an intense transition in all three clusters that blue shifts on cooling to 77 K (as do $\sigma \rightarrow \sigma^*$ transitions in dinuclear metal–metal bonded carbonyls) is assigned[24] by analogy to the "$\sigma \rightarrow \sigma^*$" transition of the cluster. Spectroscopic energies for this transition are provided in Table I, along with those for derivatives where the basal face of the cluster has been capped with the tripod [$HC(PPh_2)_3$] ligand. The energy of this transition is remarkably constant between 300 and 380 nm and seems to be characteristic for the $M_4$ grouping. On the basis of the increased d-orbital splitting in the Ir cluster (Figure 6), one might have expected the transition energy to be shifted to significantly higher energies. This may be offset by the absence of bridging CO ligands in the Ir clusters, because bridging CO groups are known to shift the energy of the $\sigma \rightarrow \sigma^*$ transition to higher energy in dinuclear cobalt carbonyl complexes.[25]

In a study of ligand effects with the $C_{3v}$ symmetry $Co_4$ clusters, substitutions were made at the basal triangular face of the cluster with the tripod ligand, at the apical Co of the cluster with an $\eta^6$-arene ligand, and at both positions simultaneously.[26] Because of the complexity of an orbital-by-orbital analysis of bonding in these highly delocalized clusters, we decided to approach the problem with a density of states (DOS) analysis similar to the description of bonding in solids. In this scheme each orbital in the MO diagram is assigned a 0.4-eV-wide Lorentzian line shape, and the resultant sum over

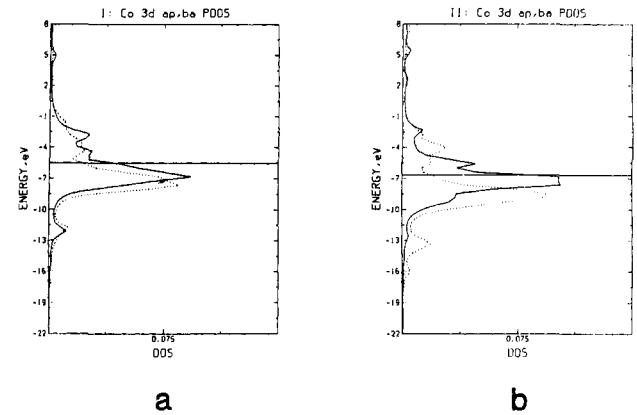


**Figure 7.** Apical- and basal-site contributions from cobalt 3d orbitals, scaled relative to the total DOS and plotted on a per-atom basis for (a) $Co_4(CO)_{12}$ and (b) $(\eta\text{-}C_6H_6)Co_4(CO)_9$; (—) apical; (···) basal. Reprinted with permission from ref 26. Copyright 1986 American Chemical Society.

all orbitals yields the total DOS. The real advantage in this method is that partial DOS plots can be constructed for a specific atomic or orbital contribution. For example, Figure 7a contains the apical- and basal-site Co 3d orbital contribution plotted on a per metal atom basis for $Co_4(CO)_{12}$ and for $(\eta\text{-}C_6H_6)Co_4(CO)_9$. The displacement of the peak for the prominent occupied Co 3d band below the Fermi energy (horizontal dashed line for the HOMO–LUMO gap) to higher binding energy for the basal cobalts suggests a greater electron-withdrawing ability of the bridging carbonyls in the basal plane. Substitution of the apical CO's by a benzene ligand destabilizes the apical cobalt d orbitals (Figure 7b), which agrees with the expected poor $\pi$-acceptor character of benzene as compared to CO. The greater acceptor ability of the bridging CO groups, regardless of basal or apical substitution, is apparent in other DOS plots for the CO groups where the binding-energy peak for electrons localized on the bridging CO are shifted to lower binding energy than those for the terminal CO groups. We believe the DOS approach has considerable merit for the analysis of orbital energy diagrams for complex molecular systems.

**Electrochemistry of Tetranuclear Cluster Compounds.** Further evidence for the delocalized character of bonding in these clusters was obtained from a con-

(25) Abrahamson, H. B.; Frazier, C. C.; Ginley, D. S.; Gray, H. B.; Lilienthal, J.; Tyler, D. R.; Wrighton, M. S. *Inorg. Chem.* **1977**, *16*, 1554.
(26) Holland, G. F.; Ellis, D. E.; Trogler, W. C. *J. Am. Chem. Soc.* **1986**, *108*, 1884.

sideration of their electrochemistry (Table I).[26,27] In the $Co_4$ series the effect of replacing either the apical or basal CO ligands with arene or tripod ligands, respectively, results in a shift of either the first anodic or the first cathodic one-electron processes to a more negative potential. Although the redox waves observed for $Co_4(CO)_{12}$ were irreversible, the tripod- and arene-substituted species generally showed chemically reversible waves for the one-electron-reduced or -oxidized radicals (Table I). Several effects may be operative. First, the tripod ligand is known to hinder fragmentation processes in the neutral cluster,[28] and it may serve a similar role in the radical cation or anion. On electronic and steric grounds, phosphorus donor ligand substitution for CO in mononuclear 17-electron compounds results in enhanced stability of radical cations.[29] Arene substitution may also enhance Co(apical)–Co(basal) bonding, as suggested by the bond lengths provided in Table I and by earlier extended Hückel calculations.[30] The potential shifts are additive, i.e., the negative potential shift in the species with both basal tripod and apical arene ligands equals the sum of the corresponding shifts in the two monosubstituted species.

From X$\alpha$ calculations of $(\eta\text{-}C_6H_6)Co_4(CO)_9$, $Co_4(CO)_9[(PH_2)_3CH]$, and $(\eta\text{-}C_6H_6)Co_4(CO)_6[(PH_2)_3CH]$, there was no apparent correlation between the redox potentials and either the HOMO or LUMO orbital energies. This contrasts with the correlations observed in mononuclear systems.[31] An excellent linear correlation (correlation coefficient 0.997) was obtained with the volume-integrated cluster-core charge for the $Co_4$ unit (Table I). Additivity of ligand effects, regardless of the site of substitution, and the correlation between net cluster-core charges and redox potentials support the notion that metal clusters behave as delocalized sources and sinks of electrons. The lack of correlation between cluster HOMO energies and redox potentials may result because the energy of an individual orbital, such as one localized on an apical cobalt, does not reflect gross molecular properties. In mononuclear complexes, which usually contain metal-localized HOMOs and LUMOs, frontier orbital energies adequately represent metal-centered oxidations and reductions.[31]

**Kinetics of CO Substitution in Metal Cluster Complexes.** Mechanistic data for the $M_4(CO)_{12}$ clusters (M = Co, Rh, Ir) was available only for $Ir_4(CO)_{12}$, where CO substitution occurs by a two-term rate law with a dominant second-order term for phosphorus nucleophiles.[32] Substitution in $Ir_4(CO)_{11-z}L_z$ ($z$ = 1–3) occurs primarily by a dissociative route,[32,33] when the entering ligand, L, is a phosphorus donor. The mechanism of CO substitution in $Co_4(CO)_{12}$ and $Rh_4(CO)_{12}$ was less well understood. Exchange of CO in $Co_4(CO)_{12}$ with $^{13}CO$ and $^{14}CO$ proceeds by a dissociative path, while fragmentation to $Co_2(CO)_8$ (at high temperature and high CO pressure) follows a rate law with first- and second-order terms in CO.[34] In contrast, the reaction between $Co_4(CO)_{12}$ and L occurred too rapidly to be measured, which suggests an associative mechanism.[35] Only a lower limit could be set on the rate of CO substitution in $Rh_4(CO)_{12}$.[36] Part of the motivation for examining the series was the report that CO dissociation rates of $M_3(CO)_{12}$ clusters follow the order[37] Fe > Ru > Os. This contrasts with trends observed in periodic series of mononuclear complexes where an enhanced reactivity for second-row transition metals usually obtains.

When the reaction between $Co_4(CO)_{12}$ and $PPh_3$ was examined with a combination of stopped-flow and low-temperature methods,[38] we found that the CO substitution process showed an induction period that varied from 1 to 15 s at 28 °C to as long as 2 h at −43 °C. Although this reaction may proceed by electron-transfer catalysis, as for example in $H_3CCCo_3(CO)_9$,[39] the intrinsic reactivity of $Co_4(CO)_{12}$ is low. In contrast the rate of CO substitution in $Rh_4(CO)_{12}$ is well-behaved and both mono- and disubstituted products form according to a second-order rate law $k[Rh_4(CO)_{12}][PPh_3]$. While it was apparent that the reactivity of $Rh_4(CO)_{12}$ exceeded that of $Co_4(CO)_{12}$ and $Ir_4(CO)_{12}$, a quantitative comparison was precluded because of the autocatalytic nature of the $Co_4(CO)_{12}$ reactions. Therefore, the stabilized tripod-substituted clusters were examined.

The substitution of CO in $M_4(CO)_9[HC(PPh_2)_3]$ clusters (M = Co, Rh, and Ir) proceeds with a variety of phosphorus donor ligands, L, to yield the apical-substituted $M_4(CO)_8[HC(PPh_2)_3]L$. Kinetic studies[40] show that two-term rate laws $(k_1 + k_2[L])[M_4(CO)_9[HC(PPh_2)_3]]$ are observed for M = Co and Rh, whereas for Ir the second-order term dominates for all L except $^{13}CO$. Activation parameters for the $k_1$ terms ($\Delta H^\ddagger_1$ = 22–26 kcal/mol and $\Delta S^\ddagger_1$ = 0–23 cal mol$^{-1}$ K$^{-1}$) agree with a CO dissociative mechanism for the $k_1$ process. Activation parameters for the $k_2$ terms ($\Delta H^\ddagger_2$ = 5–14 kcal/mol and $\Delta S^\ddagger_2$ = −20 to −45 cal mol$^{-1}$ K$^{-1}$) and the dependence of rate on incoming nucleophile suggest an associative mechanism for CO substitution, where L attacks an apical metal atom of the cluster. Rates of CO substitution in $M_4(CO)_9[HC(PPh_2)_3]$ are generally

(27) Rimmelin, J.; Lemoine, P.; Gross, M.; de Montauzon, D. *Nouv. J. Chim.* **1983**, *7*, 453. Rimmelin, J.; Lemoine, P.; Gross, M.; Bahsoun, A. A.; Osborn, J. A. *Ibid.* **1985**, *9*, 181.

(28) (a) Arduini, A. A.; Bahsoun, A. A.; Osborn, J. A.; Voelker, C. *Angew. Chem., Int. Ed. Engl.* **1980**, *19*, 1024. (b) Bahsoun, A. A.; Osborn, J. A.; Voelker, C.; Bonnet, J. J.; Lavigne, G. *Organometallics* **1982**, *1*, 1114. (c) Bahsoun, A. A.; Osborn, J. A.; Kintzinger, J.-P.; Bird, P. H.; Siriwardane, U. *Nouv. J. Chim.* **1984**, *8*, 125.

(29) Trogler, W. C. *Int. J. Chem. Kinet.* **1987**, *19*, 1025. Trogler, W. C. In *Organometallic Radical Processes*; Trogler, W. C., Ed.; Elsevier: Amsterdam, 1990, pp 306–337.

(30) Elian, M.; Chen, M. M. L.; Mingos, D. M. P.; Hoffmann, R. *Inorg. Chem.* **1976**, *15*, 1148.

(31) Sarapu, A. C.; Fenske, R. F. *Inorg. Chem.* **1975**, *14*, 247. Bursten, B. E. *J. Am. Chem. Soc.* **1982**, *104*, 1299. Bursten, B. E.; Darensbourg, D. J.; Kellogg, G. E.; Lichtenberger, D. L. *Inorg. Chem.* **1984**, *23*, 4361.

(32) Karel, K. J.; Norton, J. R. *J. Am. Chem. Soc.* **1974**, *96*, 6812. Dahlinger, K.; Falcone, F.; Poë, A. J. *Inorg. Chem.* **1986**, *25*, 2654. Sonnenberger, D. C.; Atwood, J. D. *Inorg. Chem.* **1981**, *20*, 3243. Stuntz, G. F.; Shapley, J. R. *J. Organomet. Chem.* **1981**, *213*, 389.

(33) Sonnenberger, D. C.; Atwood, J. D. *J. Am. Chem. Soc.* **1982**, *104*, 2113. Sonnenberger, D. C.; Atwood, J. D. *Organometallics* **1982**, *1*, 694. Darensbourg, D. J.; Baldwin-Zuchke, B. J. *J. Am. Chem. Soc.* **1982**, *104*, 3906.

(34) Cetini, G.; Gambino, I.; Sappa, E.; Vaglio, G. A. *Ric. Sci.* **1967**, *37*, 430. Bor, G.; Dietler, U. K.; Pino, P.; Poë, A. J. *J. Organomet. Chem.* **1978**, *154*, 301. Keeley, D. F.; Johnston, R. E. *J. Inorg. Nucl. Chem.* **1959**, *11*, 33. Darensbourg, D. J.; Peterson, B. S.; Schmidt, R. E., Jr. *Organometallics* **1982**, *1*, 306.

(35) Darensbourg, D. J.; Incorvia, M. J. *Inorg. Chem.* **1980**, *19*, 2585.

(36) Norton, J. R.; Collman, J. P. *Inorg. Chem.* **1973**, *12*, 476.

(37) Poë, A. J.; Sekhar, V. C. *Inorg. Chem.* **1985**, *24*, 4376.

(38) Kennedy, J. R.; Basolo, F.; Trogler, W. C. *Inorg. Chim. Acta* **1988**, *146*, 75.

(39) Hinkelmann, K.; Heinze, J.; Schacht, H.-T.; Field, J. S.; Vahrenkamp, H. *J. Am. Chem. Soc.* **1989**, *111*, 5078 and references therein.

(40) Kennedy, J. R.; Selz, P.; Rheingold, A. L.; Trogler, W. C.; Basolo, F. *J. Am. Chem. Soc.* **1989**, *111*, 3615.

less than in corresponding $M_4(CO)_{12}$ clusters, since the $HC(PPh_2)_3$ ligand donates electron density to the cluster (as compared to CO). This results in enhanced $\pi$-back-bonding to CO groups in the cluster, which raises the barrier to CO dissociation. Increased electron density at M, as well as the increased steric bulk of the tripod ligand, decreases the susceptibility of the cluster toward nucleophilic attack.

The $M_4(CO)_9[HC(PPh_2)_3]$ clusters (M = Co, Rh, Ir) show increased reactivity toward CO dissociation in the order Ir $\ll$ Co < Rh with relative ratios of $10^{-5}$:1:667. A dramatic decrease in reactivity for the Ir complex can be attributed to the absence of bridging carbonyls. A comparison of the data for $Ir_4(CO)_9$(tripod) and earlier data[33] for substitution in $Ir_4(CO)_{12}$ and $Ir_4(CO)_9(PPh_3)_3$ suggests that bridging carbonyl groups enhance cluster lability, as originally suggested by Norton and Collman.[36] However, the $10^4$ increase occurs in CO dissociation rates. Associative attack does not share in the rate enhancement. Bridging CO groups might stabilize the excess d$\pi$ electron density,[41] which develops in the cluster as a $\pi$-acceptor CO ligand dissociates. Bridging CO groups should also weaken $\pi$-back-bonding to the terminal CO groups, which could result in enhanced dissociative lability. For example, the X$\alpha$ calculations[26] for $Co_4(CO)_{12}$ show a small (-0.18) negative charge for the apical carbonyls in comparison to the basal terminal (-0.27) and edge-bridging (-0.34) carbonyls. This may also explain the anomalous trend Fe > Ru > Os observed[37] for CO dissociation in the $M_3(CO)_{12}$ family. Only the Fe cluster contains bridging CO groups.

A striking difference between the reactivity of mononuclear carbonyl complexes and the cluster systems is the presence of a facile associative path for CO substitution in the latter compounds. A dinuclear structure does not seem to be sufficient for introducing an associative mechanism, since the $M_2(CO)_{10}$ (M = Mn, Re) complexes react predominantly by CO dissociative paths.[42] The presence of bridging CO groups also does not appear to be a key factor in controlling the rate of associative CO substitution. In a relative sense the associative path becomes dominant as one descends the periodic table. This could arise from increased steric accessibility for nucleophilic attack as cluster size increases and the increased positive $M_4$ core charge (Table I) on descending the triad. For $M_4(CO)_9[HC(PPh_2)_3]$ the associative rates of substitution increase in the order Ir < Co $\ll$ Rh with ratios of $10^{-3}$:1:$10^6$. Substitution of CO groups in the cluster by phosphine ligands generally leads to a decrease in associative substitution reactions because of increased electron density (decreased electrophilicity) at the metal core. The magnitude of this decrease is not as pronounced as in mononuclear systems and can be attributed to a possible site of nucleophilic attack (e.g., apical position) distant from the site of tripod ligation (i.e., basal position) in a cluster.

When triangular faces of metal atoms occur, then the lowest lying metal localized acceptor orbital is the $\sigma_{cp}$* orbital for the cyclopropane-like $\sigma$-bonding network, as discussed for $M_3(CO)_{12}$ clusters. This orbital is directed out the edge of the cluster as shown in Figure 2 and may be accessible to attack by a nucleophile. Indeed, one of the unusual features observed in kinetics studies of $M_3(CO)_{12}$ clusters was the presence of facile associative reaction paths.[43] The energy of the lowest acceptor orbital follows the order $Co_4$ < $Rh_4$ < $Ir_4$, as inferred from optical spectroscopy, and the electrochemical reduction potential measurements, $E_{pc}$ (Table I), parallel this trend. Metal–carbonyl bond strengths inferred from bond-length data (Table I), M–$C_{ap}$, or from the trend in rates of dissociative CO loss discussed earlier appear to follow the order Rh < Co < Ir. Steric accessibility for nucleophilic attack should also parallel the metal–metal bond lengths, $M_{ap}$–$M_{ba}$ Co $\ll$ Ir $\sim$ Rh. A weakened metal–metal bond should enhance the susceptibility of clusters to associative attack because metal–ligand bonding in the transition state will reduce the number of electrons involved in cluster bonding. Poë has suggested that opening of the cluster and CO rearrangement concomitant with nucleophilic attack can produce a ligand-rich intermediate that obeys the electron counting rules.[43]

**Concluding Remarks.** The large number of valence orbitals in polynuclear metal–metal-bonded complexes, coupled with their highly delocalized character, leads to a breakdown of simple orbital descriptions of ground- and excited-state reactivities. We have shown how partial density of states analyses and difference electron density plots offer a partial solution to these problems, when combined with a traditional molecular orbital approach. Volume-integrated charge densities for the cluster core seem useful in understanding net redox properties of cluster compounds, and difference density plots provide a useful picture of excited-state bonding changes. The description of the thermal reactivity of cluster compounds, however, needs further refinement.

A striking difference between the reactivity of mononuclear and polynuclear systems is the increased importance of associative reaction mechanisms in cluster systems. Whether this originates from the availability of low-lying acceptor orbitals, the availability of metal–metal bond homolysis to produce open cluster frameworks, or other factors remains to be established. Both the partial density of states analyses and charge analyses underscore the importance of bridging CO groups in polarizing the charge distribution in metal cluster cores. While there is a connection between an enhanced rate for CO dissociation from clusters and the presence of bridging CO groups, the role of terminal-bridging CO interconversions in reaction mechanisms needs further definition. Other problems of current interest to our group concern the effect of the removal of an electron from the highest occupied orbital or the effect of the addition of an electron to the lowest unoccupied orbital of a closed-shell cluster complex on its reactivity. For example, oxidation[44] of $Fe_2(CO)_7(\mu$-$PPh_2)^-$ by one electron increases the rate of associative CO substitution by $10^5$, and one-electron reduction[45] of $Rh_4(CO)_9$(tripod) accelerates dissociative loss of CO by $>10^3$. In addition, we are making an effort to define

(41) Shriver, D. F. *Chem. Br.* **1972**, *8*, 419. Kristoff, J. S.; Shriver, D. F. *Inorg. Chem.* **1974**, *13*, 499.
(42) Atwood, J. D. *Inorg. Chem.* **1981**, *20*, 4031. Schmidt, S. P.; Trogler, W. C.; Basolo, F. *Inorg. Chem.* **1982**, *21*, 1699. Muetterties, E. L.; Burch, R. R.; Stolzenberg, A. M. *Annu. Rev. Phys. Chem.* **1982**, *33*, 89.
(43) Poë, A. J. *Int. J. Chem. Kinet.* **1988**, *20*, 467. Poë, A. J. *Pure Appl. Chem.* **1988**, *60*, 1209. Brodie, N. M. J.; Poë, A. J. *J. Organomet. Chem.* **1990**, *383*, 531.
(44) Baker, R. T.; Calabrese, J. C.; Krusic, P. J.; Therien, M. J.; Trogler, W. C. *J. Am. Chem. Soc.* **1988**, *110*, 8392.
(45) Phillips, J. R.; Trogler, W. C., to be published.

mechanisms of redox-induced metal-metal bond breaking.

Because the connection between the electronic structure and reactivity of molecular clusters of increasing size and small metal particles bears on problems relevant to catalysis and materials science, a continued interest in cluster research seems likely. Both experimental and theoretical chemists will be challenged to develop reliable methods for elucidating the chemistry and electronic structures of large clusters.

*This work is based on research sponsored by the National Science Foundation. The efforts of the many student and faculty collaborators in the references cited are gratefully acknowledged.*

# Computer Modeling of the Interactions of Complex Molecules

PETER A. KOLLMAN* and KENNETH M. MERZ, JR.†

*Department of Pharmaceutical Chemistry, University of California, San Francisco, San Francisco, California 94143*

*Received October 9, 1989 (Revised Manuscript Received April 3, 1990)*

The usefulness of computer-based approaches to simulate the properties of molecules is now accepted in most areas of chemistry. The accuracy with which one can approximate the solution to the Schrödinger equation ab initio for small molecules is constantly increasing,[1] and semiempirical molecular orbital methods have made useful contributions to medium-sized molecules.[2] Computer simulation methods[3] have led to exciting new insights into the properties of condensed phases of molecules. The major focus of this Account is on some of the advances in applications of computer approaches to biological macromolecules.

These computer-based applications can vary from the use of data bases and computer graphics to numerical calculations in the areas of molecular quantum mechanics, molecular mechanics, and statistical mechanics. The focus of our research is to understand the nature of molecular interactions in complex molecules; both numerical calculations and computer graphics methods have been used in our pursuit of this understanding. We wrote an Account some years ago,[4] and it will give a useful historical perspective to this Account.

There are three fundamental problems in the computer simulations of complex biological molecules. The first and most difficult to overcome is the "global minimum" problem. Globular proteins and nucleic acids have hundreds or even thousands of atoms and correspondingly many degrees of conformational freedom. Even if one could exhaustively search conformational space, one still needs to correctly evaluate and rank the relative free energies of all the conformations. This is currently impossible even for systems of ~100 atoms.

Secondly, the study of complex molecules with energy calculations requires molecular mechanics methods. This stands in contrast to studies of small molecules in the gas phase where Schrödinger's equation can be solved to an adequate degree of accuracy to represent the structure, reactivity, and energies of the molecules. Can we say anything useful with such simple approaches to represent the structure and complexation energies of systems?

Thirdly, the quantity of relevance in understanding the energetics of complex systems is the free energy; what can we say about free energies of such systems?

In the last five years there have been useful advances in conformational searching methods to overcome the global minimum problem. There is a growing acceptance that the question about the usefulness of molecular mechanics methods should be answered definitively yes, and there have been tremendous advances in our ability to calculate free energy differences to make direct and meaningful contact with experiment. This Account will focus on our contributions in these area of research, but will conclude that some other applications to demonstrate that various computational methods can be synergistic in giving useful qualitative insight into complex systems. With the latter we reinforce a major theme of our previous Account.

## Conformational Searching and the Global Minimum Problem

Development of methods for conformational searching on "small" constrained systems such as crowns[5] and cyclic peptides or antibody combining loops[6,7] provides

Peter Kollman was born in Iowa City, IA, on July 24, 1944, and attended Grinnell College and Princeton University, where he received his Ph.D. in 1970, working under the supervision of Leland Allen. After a postdoctoral year in Cambridge, England, with David Buckingham, he joined the faculty of the School of Pharmacy, Department of Pharmaceutical Chemistry, University of California, San Francisco, where he is now Professor of Pharmaceutical Chemistry. He is the father of two children, Sarah and Eli, and the husband of Mercedes Acosta. This year he achieved a personal best by making 26 free throws in a row.

Kenneth Merz was born in Niagara Falls, NY, in 1959. He received his B.S. in 1981 from Washington College in Chestertown, MD, and his Ph.D. in 1985 from the University of Texas at Austin under the supervision of M. J. S. Dewar. Postdoctoral work followed, with R. Hoffmann at Cornell University and with P. Kollman at the University of California, San Francisco. In 1989 he joined the faculty at the Pennsylvania State University (University Park Campus), where he is now an Assistant Professor of both Chemistry and Molecular and Cell Biology. In 1990 he received an Office of Naval Research Young Investigator Award. His research interests lie in method development and the study of the structure and function of zinc metalloenzymes and antibiotic ionophores.

†Current address: Department of Chemistry, Pennsylvania State University, State College, PA 16802.

(1) Schaefer, H. F. *Science* **186**, *231*, 1100.
(2) Dewar, M.; Zoebisch, E.; Healy, E.; Stewart, J. *J. Am. Chem. Soc.* **1985**, *107*, 3902.
(3) McCammon, J. A.; Harvey, S. C. *Molecular Dynamics of Proteins and Nucleic Acids*; Cambrdige Univ. Press: New York, 1987.
(4) Kollman, P. *Acc. Chem. Res.* **1985**, *18*, 105.
(5) Billeter, M.; Howard, A.; Kuntz, I.; Kollman, P. *J. Am. Chem. Soc.* **1988**, *110*, 8385.
(6) Bruccoleri, R.; Karplus, M. *Biopolymers* **1987**, *26*, 137.
(7) Fine, R.; Wang, H.; Shenkin, P.; Yarmuth, N.; Levinthal, C. *Proteins* **1986**, *1*, 342.

0001-4842/90/0123-0246$02.50/0 